Pergamon

Cement and Concrete Research, Vol. 27, No. 5, pp. 785-795, 1997

0008-8846/97 $17.00 + .00

PII S0008-8846(97)00063-X

ON THE TORTUOSITY OF THE FRACTURE SURFACE IN CONCRETE

B.B. Sabir, S. Wild and M. Asili
Division of Civil Engineering, School of the Built Environment, The University of Glamorgan, Pontypridd, UK, CF37 1DL

(Refereed)
(Received August 6, 1996; in final form April 1, 1997)

ABSTRACT

This study presents the results of fracture toughness and fracture energy of concrete obtained from tests conducted on compact compression eccentrically loaded (CCEL) specimens. The fracture toughness is calculated from the critical value of the stress intensity factor, the latter being determined by a numerical procedure. The specimen geometry and testing procedure used results in a linear load-displacement relationship; the area under the resulting curve is used to determine the fracture energy with an allowance being made for the interaction that takes place between the specimen and the testing machine. The fracture energy is also determined from the critical value of the strain energy release rate which is evaluated through the fracture toughness. Several notch geometries are considered and the results show that while the fracture toughness is not influenced by the notch size, the fracture energy decreased with increasing size of notch. The test methodology and calculation procedure enabled an estimation to be made of the tortuosity effects on the fracture surface of the concrete.

Nomenclature

- a = crack length
- d = specimen depth
- E = elasticity modulus
- E_f = fracture energy per unit area of crack extension
- G_c = critical strain energy release rate
- K = stress intensity factor
- K_c = fracture toughness
- k_m = stiffness of testing machine
- P = eccentric compressive load
- W_m = energy absorbed by testing machine
- W_s = energy of fracture
- μ = Poisson's ratio

δ = deformation of testing machine
Δ = displacement at fracture

Introduction

Fracture in concrete has been the subject of research for a long time and a large number of experimental investigations have been carried out over the last decade or so directed towards a greater understanding of the process and mechanisms of fracture in cementitious materials. The principal quantities used to characterise and quantify the resistance of concrete to crack propagation, and ultimately failure, are the fracture toughness K_c, fracture energy E_f and critical crack tip opening displacement $CTOD_c$. The hope in examining fracture in concrete by evaluating K_c, E_f and $CTOD_c$ is that these quantities would prove to be strength parameters similar to compressive strength, tensile strength, etc., which can be readily available to the concrete design engineer. Unfortunately the results of investigations suggest that, in relation to the way in which these quantities are measured, the fracture toughness and fracture energy are far from being unique to the material in hand and depend on specimen geometry, dimensions of specimens and the size of the crack in the test piece prior to the commencement of testing. Contrary to the usual properties of concrete, including compressive, tensile and torsional strengths, which decrease with increasing specimen size, the fracture toughness and fracture energy are found to increase with increasing specimen size. These values increase asymptotically to levels beyond which any further increase in specimen size leads to little or no increase in the fracture toughness or the fracture energy.

It is also generally found that the fracture toughness is influenced by the size of the pre-crack. However, this variation with increasing crack size is not systematic and a whole range of different behaviours have been reported by different authors (1-6). This contrary phenomenon is generally referred to as the 'size effect' and is largely attributed to the slow micro-cracking at the aggregate-paste interface that takes place ahead of the crack tip before fracture. Attempts to modify the fracture toughness evaluation by augmenting the pre-crack length by an additional increment to account for this 'micro-processing zone' have not been entirely successful and there is currently a RILEM proposal for evaluating the fracture energy and size of the process zone by what is termed the size effect law (7). A competing proposal (8), also produced by RILEM, is the two-parameter model which assesses the fracture behaviour through the critical value of the stress intensity factor or fracture toughness KIc and the critical value of the crack tip opening displacement $CTOD_c$. Several investigations have been carried out on the basis of these proposals and a good deal of controversy exists regarding the validity and practicality of these tests (9-11). Both proposals employ the three point bend test applied to beams of sizes which render the test unsuitable and expensive in practice. The work presented in this paper is based on tests conducted on 100 mm concrete cubes, modified by introducing symmetrical notches on opposite faces, and loaded eccentrically in an Instron testing system. Except for a small initial non-linear behaviour, due to bedding-in of the load, the test results in linear load-displacement relationships with sudden and complete fracture taking place at the maximum load attained. The area under the load-displacement curve is used to determine the fracture energy, and the fracture toughness is evaluated through the stress intensity factor at maximum load. Several notch sizes were examined and the results are analysed to investigate the extent of the tortuosity of the newly created fracture surface.

Fracture Test

Compact compression eccentrically loaded (CCEL) specimens (12) were prepared by means of standard steel moulds. The concrete cubes were cured in water at 20°C for a period of 21 days at which time the notches were introduced. Symmetrical notches in the range 25-40 mm were cut on opposite faces using a specially adapted horizontal milling machine and a 1 mm thick diamond impregnated cutting disc. The samples were then returned to the curing tank until they were tested at 28 days. The test specimens were manufactured from concrete having a water/cement ratio 0.47, a cement content of 497 kg/m^3 and proportions of cement:sand:coarse aggregate of 1:1.5:2.0. The coarse aggregate was 10 mm crushed limestone. Condensed silica fume (CSF) was used in the mixes, as a partial cement replacement material, at replacement levels of 0, 4, 6, 8, 10 and 12% by mass of cement.

The tests were conducted at ambient temperature using a 250 kN Instron testing machine. The load was applied through steel bars of cross-section 6 mm × 6 mm at a constant rate of 0.4 mm/min. The load-displacement behaviour was such that, after initial bedding-in, the results showed linear relationships until sudden fracture of the test specimen into halves.

Fracture Toughness K_c

Finite element analyses of the CCEL specimens were carried out using isoparametric elements with quarter point elements employed at the crack tip (13). The results were used to evaluate the stress intensity factor K, for a unit applied load, by energy methods. The fracture toughness K_c is defined as the critical value of the stress intensity factor and was calculated from the product of K and the load which causes failure in the specimen. K_c may be used to determine the critical value of the strain energy release rate G_c, or fracture energy, from the following plane strain relationship:

$$G_c = \frac{K_c^2}{E}(1-\mu^2) \qquad (1)$$

In equation 1, E is the elasticity modulus and μ is Poisson's ratio.

Experimentally Determined Fracture Energy E_f

The testing system enabled the production of load-displacement relationships autographically. Typical curves are given in (13) and only a schematic representation is shown in Figure 1. The area under the load-displacement curve can be used to estimate the energy absorbed by the specimen up to failure provided allowance is made for the interaction that takes place between the specimen and loading machine. The displacement recorded during the fracture test is the total displacement Δ of the machine-specimen system. Figure 1 also shows the load -displacement relationship for the testing machine. This gives the machine stiffness and was

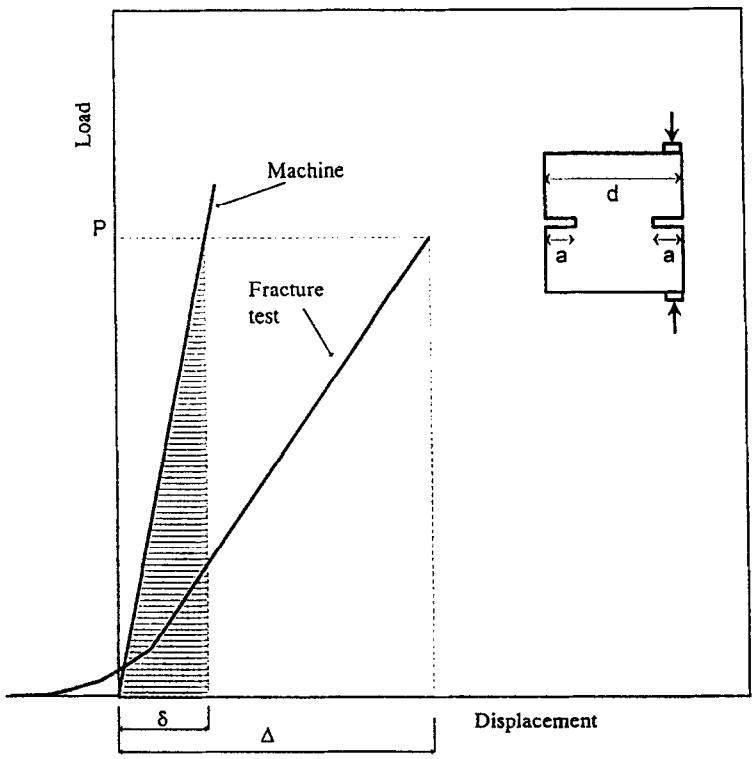

FIG. 1.
Schematics for load-displacement relationships.

obtained by compressing the loading platens (in displacement mode) against each other. Under a given load the, machine stiffness k_m is related to the deformation of the testing machine δ by

$$k_m = \frac{P(\delta)}{\delta} \tag{2}$$

Where $P(\delta)$ is the load which produces the displacement δ. The work done W_m during this deformation is given by the area under the load-displacement curve, i.e.

$$W_m = \frac{P(\delta)\delta}{2} \tag{3}$$

W_m gives the energy absorbed by the testing machine in producing the deformation δ. Substituting for the displacement δ from equation 1 into equation 2 we obtain

TABLE 1

Fracture Toughness for Specimens with 25 mm Notches

CSF (%)	P (kN)	C_v (%)	Δ (mm)	C_v (%)	K_c $MN/m^{3/2}$	C_v (%)
0	9.62	1.4	0.13	4.6	0.64	0.9
4	9.96	3.4	0.12	8.3	0.67	3.0
6	9.66	1.5	0.12	4.7	0.65	1.5
8	10.01	2.3	0.13	4.6	0.67	2.3
10	10.22	1.7	0.13	4.6	0.69	1.7
12	10.44	6.6	0.14	4.2	0.70	6.7
Mean K_c , C_v					0.67	3.4

$$W_m = \frac{P^2(\delta)}{2k_m} \tag{4}$$

If the total displacement of machine and specimen, under the load P, is Δ then the energy consumed in producing the new fracture surface is

$$W_s = 0.5P(\Delta)\Delta - \frac{P^2(\delta)}{2k_m} \tag{5}$$

The values of P and δ at fracture are output by the testing system and k_m, for a loading rate of 0.4 mm/min, was found to be 175 kN/mm. The fracture energy E_f is obtained by dividing W_s by the ligament area available for crack extension.

TABLE 2

Fracture Toughness for Specimens with 30 mm Notches

CSF (%)	P (kN)	Cv (%)	Δ (mm)	C_v (%)	K_c $MN/m^{3/2}$	C_v (%)
0	5.48	3.3	0.12	5.0	0.65	3.9
4	6.09	3.5	0.12	4.7	0.73	3.6
6	5.62	3.2	0.12	8.3	0.67	2.6
8	5.83	2.7	0.12	5.0	0.70	2.2
10	5.97	5.0	0.11	9.1	0.71	4.9
12	6.20	3.4	0.12	4.7	0.74	3.6
Mean K_c , C_v					0.70	4.9

TABLE 3

Fracture Toughness for Specimens with 35 mm Notches

CSF (%)	P (kN)	C_v (%)	Δ (mm)	C_v (%)	K_c $MN/m^{3/2}$	C_v (%)
0	2.81	4.1	0.10	5.6	0.60	4.2
4	3.09	3.0	0.10	10.0	0.66	3.5
6	2.86	5.8	0.09	6.7	0.61	5.7
8	2.88	4.1	0.08	19.9	0.62	4.1
10	2.94	4.1	0.10	17.3	0.63	4.0
12	3.00	3.2	0.10	6.0	0.64	3.6
Mean K_c , C_v					0.63	3.4

Results and Discussion

Fracture Toughness and Fracture Energy. Tables 1-4 give the failure loads, corresponding maximum displacements and the fracture toughness K_c for the series of tests performed on specimens with symmetrical notches of 25, 30, 35 and 40 mm respectively. K_c was determined from the maximum load and the stress intensity factor. The results shown are the mean values of three tests conducted for each CSF content and notch geometry. The tables also give the coefficients of variation (C_v) determined from the means and standard deviations. The values of C_v for all notch geometries are less than 5% and this suggests that, for the moderately low levels of CSF contents used, there is no significant variation of K_c with CSF content. Furthermore, if we consider the results for K_c for the entire range of CSF contents and notch geometries, the coefficient of variation, shown in Table 9, is 8.3%. This indicates that the CCEL specimens lead to insignificant variation in K_c with changes in notch size.

The results for the fracture energy E_f and critical strain energy release rate G_c are shown in Tables 5-8. It can be seen that, with the exception of a few results, the coefficient of variation is generally within the limits accepted for concrete testing. The variations in E_f and G_c with

TABLE 4

Fracture Toughness for Specimens with 40 mm Notches

CSF (%)	P (kN)	C_v (%)	Δ (mm)	C_v (%)	K_c $MN/m^{3/2}$	C_v (%)
0	1.34	5.6	0.09	6.7	0.59	4.9
4	1.29	3.6	0.07	7.9	0.56	3.7
6	1.23	3.3	0.07	8.7	0.53	2.9
8	1.35	7.4	0.07	17.3	0.59	7.7
10	1.35	5.2	0.08	12.5	0.59	5.5
12	1.36	1.1	0.08	19.9	0.59	1.0
Mean K_c , C_v					0.58	4.4

TABLE 5

Fracture Energy and Tortuosity Factors for Specimens 25 mm Notches

CSF (%)	E_f N/m	C_v (%)	G_c N/m	C_v (%)	T_f	C_t (m^{-1})
0	34.5	8.0	13.4	2.6	2.57	51.4
4	31.3	16.0	13.8	6.8	2.29	45.7
6	31.3	0.3	13.0	2.7	2.41	48.3
8	34.8	8.5	13.5	4.5	2.57	51.5
10	34.9	8.4	15.2	3.1	2.30	46.0
12	40.0	6.9	16.5	13.0	2.46	49.2
Mean values, C_v					2.43 , 5.1	48.7 , 5.2

notch depth are shown in Figure 2. CSF has a significant but inconsistent influence on the fracture energy. The influence is particularly significant for the specimens with the smaller notches. Furthermore, although both E_f and G_c converge to the same value as the notch size increases, E_f is considerably greater than G_c, particularly for short cracks. Similar trends of variations were obtained by other workers (3, 14-15), and the results of Nallathambi et al. (3) for G_c are shown in Figure 3 together with the average values (over the CSF content range) obtained in the present work.

Tortuosity of Fracture Surface. One of the problems involved in the determination of E_f is that associated with the fracture surface area to be used. Nallathambi and Karihaloo (16) estimated that, due to the tortuosity of the fracture path in their specimens, the fracture area was about 10% greater than the projected area determined from the width and depth of the specimen. Swamy (17) suggested that the true area can be several times greater than the assumed area. More recently Wollrab et al. (18) measured the tortuosity of the newly formed fracture surfaces, developed during tensile testing of edge notched specimens, using a surface imaging technique. Their results were expressed by a roughness factor which was defined as the ratio of the true surface area to the projected area. In calculating E_f in the present work the area was taken to be that of the plane section available for crack extension before fracture. It can, therefore, be

TABLE 6

Energy and Tortuosity Factors for Specimens with 30 mm Notches

CSF (%)	E_f N/m	C_v (%)	G_c N/m	C_v (%)	T_f	C_t (m^{-1})
0	29.2	8.5	13.8	6.6	2.12	53.0
4	33.7	8.0	16.3	7.1	2.07	51.7
6	30.9	13.1	13.9	6.2	2.22	55.5
8	30.4	6.7	14.5	5.7	2.10	52.5
10	28.2	10.8	16.4	9.9	1.74	43.6
12	34.1	8.7	18.4	6.8	1.86	46.4
Mean values, C_v					2.02 , 8.9	50.5 , 8.9

TABLE 7

Fracture Energy and Tortuosity Factors for Specimens with 35 mm Notches

CSF (%)	E_f N/m	C_v (%)	G_c N/m	C_v (%)	T_f	C_t (m^{-1})
0	20.5	10.0	11.8	8.1	1.73	57.8
4	21.2	12.2	13.6	5.9	1.55	51.7
6	16.7	5.1	11.7	11.6	1.44	48.1
8	14.4	23.8	11.5	7.9	1.27	42.2
10	19.7	20.6	12.9	8.6	1.51	50.4
12	19.8	5.0	14.0	6.4	1.42	47.5
Mean values, C_v					1.49, 10.3	49.6, 10.4

expected that the calculated E_f overestimates the fracture energy by a factor related to the tortuosity of the fracture surface. An estimate of the tortuosity of the fracture surface may be obtained from the relationship between the results for E_f and G_c. In this way a tortuosity factor (T_f) defined as E_f/G_c was determined for all the tests and the results are given in Tables 5-8. The results reveal that T_f is very nearly constant for a given notch size. The results also indicate that T_f ranges between 1.06 and 2.43 with a coefficient of variation for the entire range of tests conducted in the present study (see Table 9) of 31.3%. The variation in T_f with notch size may be explained by the fact that with the larger areas available for crack extension, i.e. with small notches, the advancing crack front will encounter more of the coarse aggregates which are largely responsible for the tortuosity during the crack propagation. The results show tendency for T_f to decrease with increasing CSF content. This suggests that CSF addition results in smoother fracture surfaces which, in turn, means a more brittle material behaviour during crack propagation (19). It is now well established that CSF affects the properties of concrete in two ways. In addition to the pozzolanic activity which leads to enhancement in cementitious components and hence increased strength, the CSF particles act as a filler altering the matrix structure of the concrete. The latter action results in a reduction in the porosity of the matrix in the region of the interfacial zone leading to a denser and more homogeneous transition zone (20). As the interfacial zone normally acts as the 'weak link' within concrete, the inclusion of

TABLE 8

Fracture Energy and Tortuosity Factors for Specimens with 40 mm Notches

CSF (%)	E_f N/m	C_v (%)	G_c N/m	C_v (%)	T_f	C_t (m^{-1})
0	13.3	10.6	11.0	11.5	1.20	60.3
4	10.6	9.6	9.7	6.8	1.09	54.7
6	9.1	7.0	8.8	6.3	1.04	52.1
8	10.0	20.7	10.4	14.4	0.96	48.2
10	12.3	18.0	11.1	10.5	1.09	54.7
12	11.7	21.9	11.8	21.3	0.99	49.6
Mean values, C_v					1.06 , 8.1	53.3 , 8.

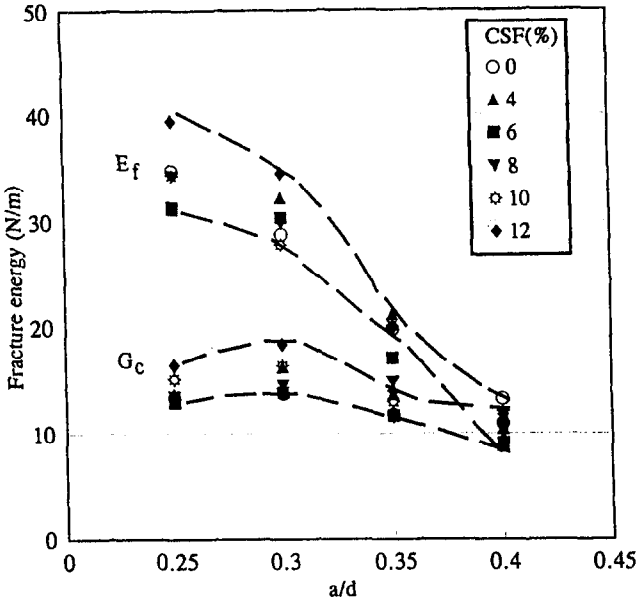

FIG. 2.
Variation of fracture energy with notch depth.

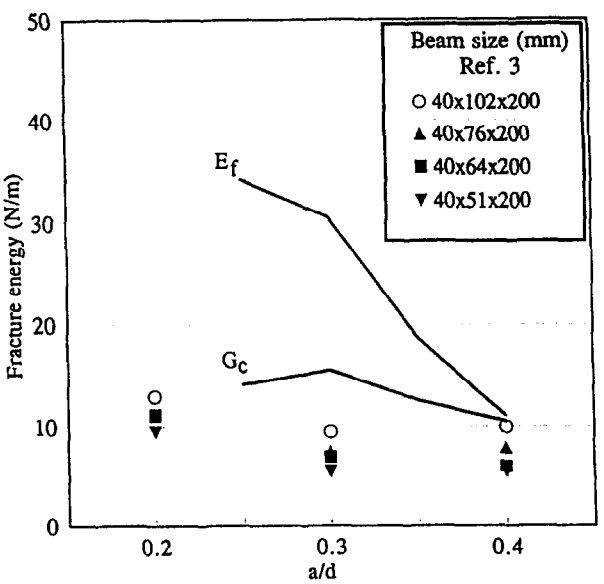

FIG. 3.
Variation of fracture energy with notch depth: results from CCEL specimens (present) and beams in flexure (Ref. 3).

TABLE 9

Statistical Data for Fracture Toughness, Tortuosity Factor and Tortuosity Coefficient

	Mean	Standard deviation	Coefficient of variation (%)
K_c	0.64	0.053	8.3
T_f	1.75	0.550	31.3
C_t	50.5	4.32	8.6

CSF results in a more effective composite action with a greater role being played by the coarse aggregate in controlling the fracture path. Whereas in normal concrete crack growth usually takes a path around the coarse aggregate, in the case of CSF concrete, because of the enhanced bond at the interface, the crack growth intercepts the aggregates themselves, breaking them and resulting in a smoother fracture surface. This behaviour was evident in the tests conducted in the present study. Other factors which will influence the extent of tortuosity is the size, strength and volume fraction of the coarse aggregate in the mix. It is worth noting that the work of Wollrab et al. (18), where only one notch geometry was considered, resulted in an average tortuosity factor of 2.1. It is also interesting to note that the concrete mixes used in (18) contained gravel (793 kg/m^3) of maximum aggregate size of 8 mm, which is similar to the aggregate proportion and maximum size, i.e. 10 mm, used in the present study. Although it is unwise to make conclusive remarks from these limited data, the results, nevertheless, show remarkable agreement. The results shown in Figure 3 exhibited considerable difference between E_f and G_c especially for the specimens with small notches. The degree of discrepency depended on the ligament length available for crack propogation and this led to the consideration of the ligament length in quantifying the tortuosity. If the tortuosity is expressed as T_f divided by the length of the ligament to give tortuosity coefficients C_t, shown in Tables 5-8, it is found that, over the entire range of tests, the coefficient of variation C_v (see Table 9) is 8.6%. If this variation is considered to be acceptable, the tortuosity coefficient C_t for the concrete examined in this study is 50.5 m^{-1}.

Conclusions

The following conclusions can be drawn from the work reported in this paper:

1. The fracture toughness evaluated from the stress intensity factor and the maximum load is not influenced by the size of the pre-notch or the levels of CSF substitutions for cement (up to 12%) used in the present study.
2. Although CSF does not significantly influence the fracture energy, the latter decreased with increasing notch size.
3. The test methodology was used to estimate tortuosity factors of the newly developed fracture surfaces and, for the concrete used in the present study, these were found to be in the range 1.1-2.4. These agreed well with the limited results obtained by Wollrab et al. (18) using a surface imaging technique.

4. The tortuosity factor decreased with increasing CSF content giving smoother fracture surfaces and indicating a more brittle material behaviour during the process of crack growth.
5. The tortuosity coefficient (tortuosity factor per unit length of ligament) remained constant for all the concretes with a value of 50.5 m^{-1}.

References

1. O.E. Gjorv, S.I. Sorensen and A. Arnesen, Notch sensitivity and fracture toughness of concrete, Cement and Concrete Research, 7, 3, 333 (1977).
2. P. Nallathambi, B.L. Karihaloo and B.S. Heaton, Effect of specimen and crack sizes, water/cement ratio and coarse aggregate texture upon fracture toughness of concrete, Magazine of Concrete Research, 36, 129, 227 (1984).
3. P. Nallathambi, B.L. Karihaloo and B.S. Heaton, Various size effects in fracture of concrete, Cement and Concrete Research, 15, 1, 117 (1985).
4. B. Hillemeier and H.K. Hilsdrof, Fracture mechanics studies on concrete composites, Cement and Concrete Research, 7, 5, 523 (1977).
5. A.P. Pak and L.P. Trapeznikov, Experimental investigations based on the Griffith-Irwin theory processes of the crack development in concrete, 5th Int Conf on Fracture, Cannes, France, 1531 (1981).
6. A.M. Brandt, Crack propogation energy in steel fibre reinforced concrete, Int Journal of Cement Composites, 2, 1, 35 (1980).
7. Draft RILEM Recommendation, Size-effect method for determining fracture energy and process zone size of concrete, Materials and Structures, 23, 123, 461 (1990).
8. Draft RILEM Recommendation, Determination of fracture parameters of plain concrete using three-point bend tests, 23, 138, 457 (1990).
9. A. Hillerborg, Results of three comparative test series for determining the fracture energy of concrete, Materials and Structures, 18, 107, 407 (1992).
10. G.V. Guinea, J. Planas and M. Elices, measurement of the fracture energy using three-point bend tests, Materials and Structures, 25, 148, 212 (1992).
11. X.Z. Hu and F.H. Wittmann, Fracture energy and fracture process zone, Materials and Structures, 23, 123, 461 (1990).
12. B.B. Sabir and M. Asili, Stress analysis of a fracture test specimen for cementitious materials, Cement and Concrete Composites, 18, 2, 141 (1996).
13. B.B. Sabir, The performance of isoparametric finite elements in stress intensity factor determination, International Journal of Fracture, 72, 259 (1995).
14. P.E. Petersson, Fracture energy of concrete: Practical performance and experimental results, Cement and Concrete Research, 10, 1, 91 (1980).
15. C.G. Go and S.E. Swartz, Energy methods for fracture toughness determination in concrete, Experimental Mechanics, 26, 3, 292 (1986).
16. P. Nallathambi and B.L. Karihaloo, Determination of specimen size independent fracture toughness of plain concrete, Magazine of Concrete Research, 38, 135, 67 (1986).
17. R.N. Swamy, Fracture mechanics applied to concrete, Developments in Concrete Technology, Applied Science Publishers, 221 (1979).
18. C. Wollrab, C. Ouyang, S.P. Shah, J. Hamm and G. Konig, The effect of specimen thickness on fracture behaviour of concrete, Magazine of Concrete Research, 48, 175, 117 (1996).
19. J.J. Mecholsky et al., Quantitative analysis of brittle fracture surface using fractal geometry, J. American Ceramic Society, 72, 1, 60 (1989).
20. A. Bentur, Microstructure, interfacial effects and micromechanics of cementitious composites, Proc. Conf. Advances in Cementitious Materials, American Ceramic Society Publications, 16, 523, (1991).